ACTA CHEMICA SCANDINAVICA 13 (1959) 241—248

Low Temperature Heat Capacities and Thermodynamic Properties of the Iron Selenides $Fe_{1.04}Se$, Fe_7Se_8 and Fe_3Se_4 from 5 to 350°K

FREDRIK GRØNVOLD

Kjemisk Institutt A, Universitetet i Oslo, Blindern, Norway

and

EDGAR F. WESTRUM, JR.

Department of Chemistry, University of Michigan, Ann Arbor, Michigan, USA

Heat capacities of three iron-selenide phases representing the tetragonal PbO-like structure with composition $Fe_{1.04}Se$ and the hexagonal and monoclinic NiAs-like structures with compositions Fe_7Se_8 and Fe_3Se_4, respectively, were measured in the range 5 to 350°K. Heat capacity values, enthalpy, and entropy increments are tabulated at different temperatures. At 298.15°K the entropies $(S^\circ - S^\circ_0)$ are 8.437 eu for $Fe_{0.5103}Se_{0.4897}$ (*i. e.*, $Fe_{1.04}Se$), 9.780 eu for $Fe_{0.4667}Se_{0.5333}$ (*i. e.*, Fe_7Se_8), and 9.554 eu for $Fe_{0.4286}Se_{0.5714}$ (*i. e.*, Fe_3Se_4). A λ-type transition with a maximum at 34°C is found in Fe_3Se_4, associated with an order-disorder process of supposedly ferrimagnetic to paramagnetic nature. The entropy increment of transition is about 2 eu per mole of Fe_3Se_4.

It has been shown by Hägg and Kindström [1] that an intermediate phase with composition FeSe and a tetragonal structure of the PbO-type exists in the iron-selenium system below a temperature between 600 and 300°C. In addition, another intermediate phase with homogeneity range from about 50 to 57.5 atomic percent selenium exists in samples quenched from 600°C. This phase has a NiAs-like structure which is hexagonal only in the iron-rich range and becomes monoclinic above 54 atomic percent selenium. By combining X-ray and density data, Hägg and Kindström concluded that the solid solution takes place by subtraction of iron atoms with increasing selenium content. Thus, the structure deforms when about 20 % of the iron lattice sites are unoccupied. This extended solid solution exists only at high temperatures and the iron-rich selenide with PbO-type structure and composition $Fe_{1.04}Se$ is formed below about 490°C according to Grønvold and Haraldsen [2].

The iron-rich composition limit of the $Fe_{1-x}Se$-phase goes towards a higher selenium content as the temperature is lowered, and at about 350°C the limit is at $Fe_{0.88}Se$ or Fe_7Se_8. Furthermore, a two-phase region is observed in the range $Fe_{0.87}Se$ to $Fe_{0.80}Se$.

As the temperature is lowered another phenomenon is also observed, *i.e.*, the ordering of the vacancies after the iron atoms. Bertaut [3] has studied the ordering process in Fe_7S_8 with NiAs-like structure and found that the decrease in internal energy for an ordered arrangement of holes compared to a random distribution is so large that all ionic defect structures are expected to have ordered distribution of the holes. This picture has to be modified for phases like the FeSe-phase which are not typical ionic compounds. It is apparent that the concentration of holes must exceed a certain value for the ordering — and thus the superstructure formation — to take place at a given temperature. With an increasing number of holes another superstructure might be formed, and so on. In case of the FeSe-phase two such superstructure phases have been established by Okazaki and Hirakawa [4], one in the composition range Fe_7Se_8 to Fe_6Se_7, the other in the range Fe_4Se_5 to Fe_3Se_4.*

In addition to the phases mentioned, an iron diselenide also exists at lower temperatures. It was found [5] in samples heat-treated for 4 months at 250°C

In respect to their magnetic properties, the iron selenides are very interesting [6]. Ferrimagnetism is associated with the FeSe-phase, with a Néel temperature at about 150°C for samples in the range $Fe_{1.00}Se$ to $Fe_{0.79}Se$. By further increase in selenium content the Néel point decreases rapidly and reaches 30°C by $Fe_{0.74}Se$. The magnetization intensity at —195°C has its maximum at $Fe_{0.89}Se$, confirming the presence of only one phase in this region. The sharp and almost linear drop on the iron-rich side can be interpreted as due to a two phase region with a paramagnetic phase with composition $Fe_{1.04}Se$, and the curved region from $Fe_{0.79}Se$ to $Fe_{0.74}Se$ as the homogeneity range of the Fe_3Se_4-phase.

More recent work by Hirone and Chiba [7] by X-ray, thermal and magnetic methods confirms the non-existence of stoichiometric FeSe and places the selenium-rich composition limit of the tetragonal phase at $Fe_{1.05}Se$ and the iron-rich limit of the hexagonal phase at $Fe_{0.88}Se$ at temperatures below 350°C. They also found ferrimagnetism associated with the hexagonal phase and a spontaneous magnetization of 0.20 Bohr magnetons. The Néel point is at 174°C and increases gradually to 192°C with increasing selenium content, and then rapidly falls to 40°C at $Fe_{0.77}Se$.

The magnetic properties of single crystals of Fe_7Se_8 and Fe_3Se_4 were studied by Hirakawa [8] using a torque magnetometer. For Fe_7Se_8 the direction of easy magnetization is in the (00.) plane at room temperature, but changes into the [001] direction below about 150°K. No such change

* Note added in proof: Okazaki (*J. Phys. Soc. Japan* **14** (1959) 112) has just reported a triclinic superstructure for Fe_7Se_8 in samples annealed at 290°C and slowly cooled. The present authors have observed a similarly deformed structure on Fe_7Se_8 samples subjected to annealing after having been in contact with the atmosphere. The sample studied here did not show any line splitting characteristic of a monoclinic or triclinic cell, and its superstructure is probably based upon an orthorhombic cell with doubled *c*-axis.

Table 1. Heat capacities of iron selenides, cal "mole"$^{-1}$ °K^{-1}.

T,°K	C_p	T,°K	C_p	T,°K	C_p
		$Fe_{1.042}Se$ (formula weight $Fe_{0.5103}Se_{0.4897}$ = 67.17 g)			
Series I		289.71	6.628	15.77	0.1864
51.58	1.639	299.16	6.692	16.89	0.2188
56.71	1.872	308.73	6.754	18.07	0.2552
63.13	2.167	318.32	6.817	19.29	0.2957
69.08	2.656	327.94	6.873	20.65	0.3412
74.43	2.805	337.51	6.928	22.30	0.3998
80.50	2.919	347.23	6.982	24.17	0.4683
87.17	3.185			26.26	0.5472
94.34	3.746	Series II		29.47	0.6758
101.47	3.686	7.02	0.023	32.30	0.7919
109.61	3.951	7.77	0.030	35.32	0.9188
118.34	4.210	8.48	0.039	38.30	1.047
127.34	4.452	9.31	0.049	41.49	1.185
136.29	4.668	10.15	0.061	45.04	1.342
144.93	4.870	11.03	0.074	48.40	1.495
154.15	5.055	11.97	0.092	54.52	1.781
163.86	5.238			60.40	2.017
173.52	5.402	Series III		64.63	2.233
182.90	5.541	5.60	0.012	67.59	2.366
192.20	5.687	6.38	0.016	70.56	2.489
201.68	5.804	7.25	0.024	73.53	2.625
211.17	5.910	8.06	0.034	76.75	2.759
223.65	6.055	8.91	0.044	80.36	2.914
232.96	6.130	9.76	0.055	83.94	3.057
242.36	6.247	10.67	0.069	87.50	3.198
251.68	6.332	11.62	0.086	91.11	3.328
261.19	6.408	12.63	0.1040	94.92	3.462
270.80	6.487	13.65	0.1274	99.11	3.604
280.33	6.559	14.67	0.1543	103.51	3.751
		Fe_7Se_8 (formula weight $Fe_{0.4667}Se_{0.5333}$ = 68.18 g)			
5.91	0.016	39.01	1.536	166.24	5.687
6.86	0.023	43.23	1.803	176.54	5.818
7.92	0.034	48.46	2.128	187.24	5.948
8.90	0.050	53.75	2.438	197.70	6.062
9.95	0.068	59.40	2.748	207.95	6.168
11.11	0.091	65.61	3.063	218.00	6.272
12.35	0.1220	68.25	3.186	228.16	6.369
13.58	0.1585	74.25	3.448	238.43	6.474
14.84	0.1994	81.67	3.766	248.51	6.570
16.13	0.2459	89.51	4.058	258.43	6.661
17.45	0.2990	97.40	4.307	268.37	6.757
18.84	0.3582	105.92	4.551	278.34	6.852
20.34	0.4296	114.67	4.773	288.43	6.951
22.02	0.5117	123.20	5.036	298.72	7.050
23.91	0.6108	131.46	5.133	308.98	7.148
26.14	0.7353	139.76	5.287	319.12	7.253
28.86	0.8944	148.64	5.435	331.24	7.389
32.66	1.129	152.28	5.495	344.70	7.544
35.41	1.305	158.23	5.580		

Table 1 (continued)

T,°K	C_p	T,°K	C_p	T,°K	C_p
		Fe_3Se_4 (formula weight $Fe_{0.4286}Se_{0.5714}$ = 69.06 g)			
Series I		327.01	6.913	53.74	2.165
		337.29	6.890	59.00	2.472
81.54	3.621	347.55	6.898	64.70	2.795
88.16	3.899			70.75	3.103
95.16	4.152	Series II		77.06	3.405
102.57	4.397			83.85	3.713
110.73	4.651	5.57	0.009	274.20	7.149
119.66	4.892	6.70	0.014	283.64	7.269
129.18	5.128	7.58	0.019	291.43	7.392
138.85	5.331	8.53	0.025	297.63	7.513
148.51	5.545	9.62	0.034	301.85	7.587
159.09	5.731	10.68	0.045	304.07	7.629
169.51	5.907	11.72	0.058	305.72	7.666
180.21	6.064	12.77	0.0737	306.83	7.678
190.88	6.212	13.85	0.0922	307.93	7.647
194.78	6.266	14.99	0.1171	309.03	7.608
204.34	6.373	16.23	0.1467	310.14	7.552
213.76	6.501	17.62	0.1856	311.24	7.446
223.01	6.600	19.11	0.2333	312.33	7.342
232.23	6.699	20.69	0.2906	313.42	7.228
241.53	6.804	22.44	0.3607	314.52	7.145
250.85	6.903	24.45	0.4500	316.19	7.057
260.04	6.996	26.82	0.5638	318.42	6.992
269.14	7.099	29.55	0.7079	320.66	6.956
278.38	7.212	32.71	0.8847	322.91	6.936
287.76	7.349	36.30	1.097	325.16	6.920
297.22	7.524	40.51	1.353	329.10	6.903
306.81	7.612	44.84	1.620	336.77	6.893
316.74	7.088	49.04	1.881	346.44	6.896

was observed for Fe_3Se_4. The saturation magnetizations at liquid air temperature for Fe_7Se_8 and Fe_3Se_4 were 68 and 80 gauss cm^{-3}, respectively.

The structural and magnetic properties of the iron selenides are thus rather sensitive to changes in temperature, and in order to get a further understanding of the causes of these changes, a thermodynamic study of the iron-selenium system is being carried out. In this paper will be reported the results of heat-capacity measurements on three single-phase samples, one representing the tetragonal FeSe-phase with composition $Fe_{1.042}Se$, and two others representing the $Fe_{1-x}Se$ phase with NiAs-like structure and compositions Fe_7Se_8 and Fe_3Se_4, or $Fe_{0.875}Se$ and $Fe_{0.750}Se$, respectively.

EXPERIMENTAL

A. Preparation of the samples. The iron selenides were synthesized from high purity iron and selenium. "Ferrum reductum pro analysi" from Merck was reduced with dry purified hydrogen gas at 1 000°C until constant weight was attained. A spectrographic analysis showed the presence of about 0.01 % Ni and Si and about 0.001 % Mn. The high-purity selenium was a gift from Bolidens Gruvaktiebolag, and contained these

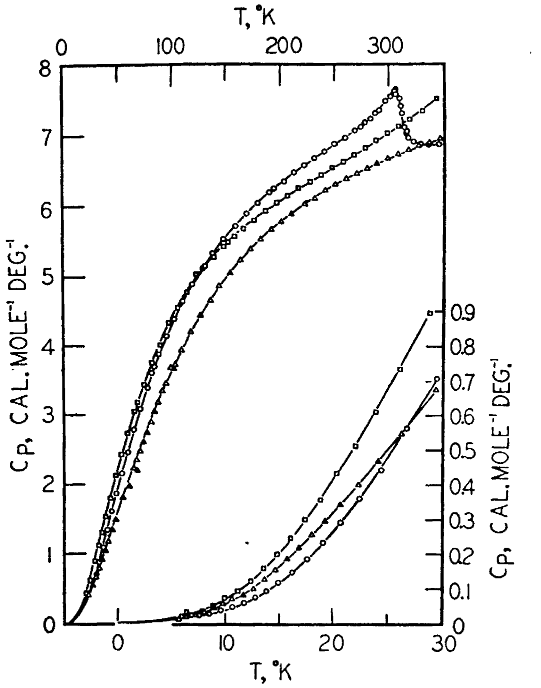

Fig. 1. Heat capacities of iron selenides on a gram formula weight basis: △ represent $Fe_{0.5103}Se_{0.4897}$, □ represent $Fe_{0.4667}Se_{0.5333}$ and ○ represent $Fe_{0.4286}Se_{0.5714}$.

impurities (in ppm) according to their analysis: Cl(2), Fe(0.8), K(0.3), Na(0.4), non-volatile matter (12). The following elements were not detected (the numbers indicate the sensitivity limit in ppm): Ag(0.03), Al(0.3), As(1), Bi(0.1), Ca(1), Cr(0.3), Cu(0.1), Hg(0.5), Mg(0.3), Mn(0.1), Ni(0.3), Pb(0.3), S(5), Sb(1), Si(1), Sn(0.3), Te(1), Zn(1).

Accurately-weighed quantities of the elements corresponding to the compositions $FeSe_{0.96}$, Fe_7Se_8 and Fe_3Se_4 were heated in evacuated and sealed silica tubes. Because of the transitions in the solid selenides which sometimes causes cracking of the silica tubes on cooling, the silica tubes were put into larger silica tubes which were also evacuated and sealed. The samples were fused for 4 h at 1 050°C in an electric muffle furnace, cooled to room temperature and fragmented under dry nitrogen in an agate mortar. They were then homogenized at 350°C for 30 days and cooled down to room temperature over another 30 days. By means of X-ray powder photographs the samples were proved to be of identical nature to those obtained earlier [2].

B. *Cryostat and calorimeter.* The Mark I cryostat and technique employed for low-temperature adiabatic calorimetry are being described elsewhere [9]. The copper calorimeter (laboratory designation W-7) has a capacity of 40.33 cm^3; it is gold-plated inside and out and has only four vanes. A separate series of measurements were carried out to determine the heat capacity of the empty calorimeter, using the same thermometer and heater and exactly the same amount of indium-tin solder for sealing and Apiezon-T grease for thermal contact with the thermometer and heater. It represented from 11 to 35 % of the total heat capacity observed.

Temperatures were measured with a capsule-type platinum resistance thermometer (laboratory designation A-3) contained in an axial well in the calorimeter. A 150-ohm constantan heater was wound on a cylindrical copper tube surrounding the resistance thermometer. The thermometer has been calibrated by the National Bureau of Standards, and the temperatures are judged to correspond with the thermodynamic temperature scale within 0.03°K from 10 to 90°K and within 0.04°K from 90 to 350°K. Precision is considerably better, and the temperature increments are probably correct to a millidegree after corrections for quasi-adiabatic drift.

The thermometer resistance and the power input were measured with a calibrated White double-potentiometer, calibrated resistances and a calibrated standard cell. An electric timer, operated by a calibrated tuning fork and amplifier, was automatically started at the beginning of the heating period and stopped at the end. The calorimeter was loaded with sample and evacuated, and helium was added at 4 cm Hg pressure at about 25°C to provide thermal contact between sample and calorimeter. It was then sealed, placed in the cryostat and cooled. The mass of sample used was 107.795 g $Fe_{1.04}Se$, 118.961 g Fe_7Se_8 and 132.015 g Fe_3Se_4.

RESULTS

The heat-capacity determinations are listed in Table 1 in chronological order, and expressed in terms of the thermochemical calorie, defined as 4.1840 abs joules. The ice point is taken to be 273.15°K, and the atomic weights of iron and selenium as 55.85 and 78.96, respectively. The data are expressed in terms of one mole of mixture ("mole"), equivalent to the gram formula weight of Fe_ySe_{1-y}; *i.e.*, 67.17 g $Fe_{1.04}Se$, 68.18 g Fe_7Se_8 and 69.06 g Fe_3Se_4. An analytically-determined curvature correction for the finite temperature increments was applied to the observed values of $\Delta H/\Delta T$. The approximate temperature increments can usually be inferred from the adjacent mean temperatures in Table 1.

The heat-capacity *versus* temperature curves are shown in Fig. 1. For $Fe_{1.04}Se$ it has the usual sigmoid shape up to 350°K, while for Fe_7Se_8 the curve shows pretransition effects and for Fe_3Se_4 a transition actually takes place at about 307°K or 34°C.

Values of C_p, $S°—S_0^\circ$ and $(H°—H_0^\circ)/T$ for the three samples are listed in Table 2 at selected temperatures. The reason for not giving the free-energy function is the uncertainty about complete ordering. The enthalpy and entropy increments were computed by numerical integration, using graphically interpolated values of heat capacity. The heat-capacity values are considered to have a probable error of 0.1 % above 25°K and 1 % at 10°K. The effects of nuclear spin and of isotope mixing are not included in the entropy function. The estimated probable error in the entropy and enthalpy functions is 0.1 % above 100°K, but some of the values are given to an additional digit because of their significance when the entropies or enthalpies at different temperatures or compositions are compared.

The entropy increment associated with the λ-transition in Fe_3Se_4 at 34°C is about 2 cal mole^{-1} deg^{-1}. The transition temperature corresponds to that found [6,7] for the change from paramagnetism to ferrimagnetism in $Fe_{0.74}Se$ and the nature of the transition seems thus established.

It is known from X-ray work [4] that the structure of Fe_3Se_4 has an ordered distribution of vacancies, just as Fe_7S_8[3], Cr_3S_4[10] and $Ni_{0.80}Se$[11], but less is known about the valence states of the atoms. According to the electrostatic treatment of Yosida [12], Bertaut [3] and Lotgering [13], the distribution of Fe^{2+}

Table 2. Thermodynamic properties of iron selenides, cal "mole"$^{-1}$ °K^{-1}.

	$Fe_{1.042}Se$ (formula weight $Fe_{0.5103}Se_{0.4897}$ = 67.17 g)			Fe_7Se_8 (formula weight $Fe_{0.4667}Se_{0.5333}$ = 68.18 g)			Fe_3Se_4 (formula weight $Fe_{0.4286}Se_{0.5714}$ = 69.06 g)		
T, °K	C_p	$S°-S°_0$	$\frac{H°-H°_0}{T}$	C_p	$S°-S°_0$	$\frac{H°-H°_0}{T}$	C_p	$S°-S°_0$	$\frac{H°-H°_0}{T}$
10	0.058	0.0195	0.0146	0.069	0.0230	0.0172	0.037	0.0125	0.0093
15	0.164	0.0606	0.0448	0.205	0.0739	0.0549	0.117	0.0405	0.0302
20	0.319	0.1284	0.0934	0.412	0.1597	0.1170	0.265	0.0928	0.0690
25	0.500	0.2186	0.1563	0.671	0.2787	0.2012	0.475	0.1736	0.1284
30	0.698	0.3269	0.2297	0.963	0.4264	0.3035	0.733	0.2824	0.2072
35	0.905	0.4499	0.3113	1.278	0.5984	0.4200	1.021	0.4167	0.3025
40	1.120	0.5849	0.3990	1.600	0.7901	0.5474	1.322	0.5725	0.4110
45	1.341	0.7295	0.4913	1.914	0.9967	0.6818	1.631	0.7460	0.5294
50	1.567	0.8825	0.5876	2.221	1.214	0.8205	1.940	0.9339	0.6550
60	2.023	1.208	0.7888	2.781	1.670	1.1015	2.530	1.340	0.9190
70	2.473	1.554	0.9975	3.266	2.136	1.3769	3.065	1.771	1.1878
80	2.897	1.912	1.2085	3.699	2.601	1.6404	3.550	2.213	1.4532
90	3.289	2.277	1.4185	4.071	3.059	1.8906	3.968	2.656	1.7102
100	3.636	2.642	1.6231	4.385	3.504	2.1246	4.319	3.092	1.9540
110	3.962	3.004	1.8211	4.658	3.935	2.3427	4.626	3.519	2.1831
120	4.253	3.361	2.0118	4.896	4.351	2.5457	4.901	3.933	2.3981
130	4.516	3.712	2.1945	5.105	4.751	2.7347	5.149	4.336	2.6004
140	4.755	4.056	2.3689	5.291	5.136	2.9107	5.372	4.726	2.7905
150	4.973	4.391	2.5354	5.457	5.507	3.0750	5.560	5.103	2.9694
160	5.167	4.718	2.6938	5.602	5.864	3.2286	5.750	5.468	3.1377
170	5.341	5.037	2.8445	5.736	6.208	3.3723	5.913	5.822	3.2963
180	5.499	5.347	2.9876	5.860	6.539	3.5071	6.060	6.164	3.4458
190	5.642	5.648	3.1236	5.975	6.859	3.6340	6.201	6.496	3.5871
200	5.775	5.941	3.2528	6.084	7.169	3.7538	6.333	6.817	3.7211
210	5.898	6.226	3.3759	6.190	7.468	3.8673	6.456	7.129	3.8485
220	6.013	6.503	3.4932	6.292	7.758	3.9752	6.571	7.432	3.9696
230	6.123	6.772	3.6051	6.392	8.040	4.0781	6.682	7.727	4.0851
240	6.226	7.035	3.7122	6.488	8.314	4.1765	6.788	8.013	4.1956
250	6.316	7.291	3.8146	6.583	8.581	4.2708	6.894	8.293	4.3014
260	6.400	7.541	3.9124	6.677	8.841	4.3616	7.002	8.565	4.4032
270	6.479	7.784	4.0061	6.772	9.095	4.4491	7.106	8.831	4.5014
280	6.556	8.021	4.0958	6.869	9.343	4.5338	7.222	9.092	4.5964
290	6.629	8.252	4.1819	6.967	9.586	4.6160	7.368	9.348	4.6894
300	6.698	8.478	4.2646	7.062	9.823	4.6959	7.551	9.600	4.7816
350	6.997	9.534	4.6344	7.603	10.951	5.0713	6.897	10.697	5.1229
273.15	6.504	7.859	4.0348	6.814	9.174	4.4762	7.138	8.914	4.5318
298.15	6.685	8.437	4.2497	7.045	9.780	4.6814	7.515	9.554	4.7645

and Fe^{3+} ions in $Fe_{1-x}Se$ in the planes I and II normal to the c-axis of the NiAs-like structure is (when ϱ designates the fraction of Fe^{3+} ions in plane I, and all vacancies are in plane II):

Plane I	Plane II
$(\frac{1}{2}-2x\,\varrho)Fe^{2+} + 2x\varrho Fe^{3+}$	$(\frac{1}{2}-x-2x[1-\varrho])Fe^{2+} + 2x(1-\varrho)Fe^{3+}$

On the basis of spin-only magnetism the magnetic moment of Fe_7Se_8 resulting from antiparallel spin arrangement between lattice I and II is calculated to vary between 0.29 and 0.86 Bohr magnetons per iron atom as ϱ goes from 0 to 1, *i.e.*, as the number of Fe^{3+} ions in lattice I increases from zero to its maximum value. By assuming all Fe^{3+} ions and vacancies to be located in the same plane, the experimentally found moment of 0.2 Bohr magnetons is reasonably well explained.

For Fe_3Se_4 the same model predicts magnetic moments of 1.33 to 2.0 Bohr magnetons per iron atom as ϱ goes from its minimum value 0.5 (corresponding to equipartition of Fe^{3+} ions between lattice I and II) to its maximum value 1.0, when all Fe^{3+} ions are in lattice I. The magnetic measurements [6] are not in agreement with this, however, as the observed moment of Fe_3Se_4 is only 0.1 Bohr magneton. This shows that strong interactions are present between the paramagnetic ions and their neighbors so that the electrostatic description has to be modified.

Acknowledgment. The authors thank Bolidens Gruvaktiebolag for a generous supply of selenium and Roger Berg and Paul (Te Fu) Chang for assistance in the calorimetric measurements. One of us (F. Grønvold) expresses his appreciation to the *Nansen Foundation* for assistance. The partial support of the *Division of Research of the U. S. Atomic Energy Commission* is gratefully acknowledged.

REFERENCES

1. Hägg, G. and Kindström, A.-L. *Z. physik. Chem.* **B22** (1933) 453.
2. Haraldsen, H. and Grønvold, F. *Tidsskr. Kjemi, Bergvesen, Met.* **10** (1944) 98; *Structure Reports for 1942–1944*, **9** (1955) 97; and unpublished results.
3. Bertaut, F. *Acta Cryst.* **6** (1953) 557; *J. phys. radium* **15** (1954) 77S.
4. Okazaki, A. and Hirakawa, K. *J. Phys. Soc. Japan* **11** (1956) 930.
5. Tengnér, S. *Z. anorg. u. allgem. Chem.* **239** (1938) 126.
6. Hirone, T., Maeda, S. and Tsuya, N. *J. Phys. Soc. Japan* **9** (1954) 496.
7. Hirone, T. and Chiba, S. *J. Phys. Soc. Japan* **11** (1956) 666.
8. Hirakawa, K. *J. Phys. Soc. Japan* **12** (1957) 929.
9. Westrum, E. F. Jr. and Beale, A. F. Jr. *J. Am. Chem. Soc. (To be published).*
10. Jellinek, F. *Diss.*, Utrecht 1957; *Acta Cryst.* **10** (1957) 620.
11. Grønvold, F. *Paper presented at the 2. Nordiske Strukturmøte*, Oslo, 1955.
12. Yosida, K. *Progr. Theor. Phys. Japan* **6** (1951) 356.
13. Lotgering, F. K. *Z. physik. Chem.* **N.F. 4** (1955) 238; *Philips Research Reports* **11** (1956) 190.

Received September 30, 1958.